C24 *Arabidopsis* genomic DNA library and isolate a *Bgl*II genomic DNA fragment encoding the complete *HIC* open reading frame, and also to identify ATTS5501 expressed sequence tag (clone YAY1019) by a BLASTN homology search of the dbest database (this cDNA was provided by J. Giraudat, CNRS, Gif, France). The complete nucleotide sequences of ATTS5501 (2,073 bp), pFL30 (5,600 bp) and pFL44 (1,584 bp) inserts were determined. The *HIC* gene is identical to a region of BAC T3A4 (accession no. AC005819) on *Arabidopsis* chromosome 2. The cloned sequences pFL30 and ATTS5501 are identical in their regions of overlap. pFL44 contains an additional 123-bp mitochondrial DNA insertion from nucleotide position 482–604 (identical to part of the *Arabidopsis* mitochondrial genome sequence part B (accession number Y08502) which is also present elsewhere on chromosome 2; ref. 28). It is probable that the insertion causing the *hic* mutation occurred during the *Agrobacterium-tumefaciens*-mediated transformation process used to generate *hic*. PCR was used to confirm the presence of this mitochondrial DNA insertion in *hic* plants and its absence in C24. The *GUS* gene is inserted 89-bp 3′ of the putative *HIC* stop codon. RT–PCR was used to confirm the presence of the *GUS* insert downstream of *hic* in the same gene transcript by amplifying a fragment of DNA that spanned the two coding regions.

Generation of *HIC* antisense plants.

ATTS5501 cDNA was excised from pBluescript using *Eco*RI and ligated into pART7 (ref. 29). The resulting plasmid was digested with *Not*I to release the cDNA in the reverse orientation between the CaMV 35S RNA promoter and OCS 3′ terminator which was ligated into pART27 (ref. 29). Gene constructs were confirmed by DNA sequencing and *Agrobacterium*-mediated transformation was carried out as described[30]. The presence of the transgene in plants was verified by PCR (data not shown). RT–PCR with primers (5′-GCTAGTGGTGAACGTCATGC-3′ and 5′-ACAAAATCGTTACCGCAAG-3′ designed specifically to amplify a 1,281-bp region of the 5′ untranslated portion of the *HIC* mRNA that differs from other known *KCS*-like genes) was used to show that the level of the *HIC* gene transcript was either considerably reduced in the antisense plants (line AS3) or undetectable by this method (AS1 and AS2), in comparison with C24 plants, which gave a clear band of DNA of the expected size on agarose gel electrophoresis. Separate amplification reactions with ubiquitin-specific primers were carried out to confirm equal amounts of mRNA. Control reactions minus reverse transcriptase gave no signal.

Received 15 May; accepted 23 October 2000.

1. Woodward, F. I. Stomatal numbers are sensitive to CO_2 increases from pre-industrial levels. *Nature* **327,** 617–618 (1987).
2. Woodward, F. I. & Kelly, C. K. The influence of CO_2 concentration on stomatal density. *New Phytol.* **131,** 311–327 (1995).
3. McElwain, J. C. & Chaloner, W. G. Stomatal density and index of fossil plants track atmospheric carbon-dioxide in the paleozoic. *Ann. Bot.* **76,** 389–395 (1995).
4. McElwain, J. C., Beerling, D. J. & Woodward, F. I. Fossil plants and global warming at the Triassic–Jurassic boundary. *Science* **285,** 1386–1390 (1999).
5. Post-Beittenmiller, D. Biochemistry and molecular biology of wax production in plants. *Annu. Rev. Plant Physiol. Plant Mol. Biol.* **47,** 405–430 (1996).
6. Topping, J. F., Wei, W. B. & Lindsey, K. Functional tagging of regulatory elements in the plant genome. *Development* **112,** 1009–1019 (1991).
7. Goddijn, O. J. M., Lindsey, K., van der Lee, F. M., Klap, J. C. & Sijmons, P. C. Differential gene-expression in nematode-induced feeding structures of transgenic plants harbouring GUSA fusion constructs. *Plant J.* **4,** 863–873 (1993).
8. Yang, M. & Sack, F. D. The *too many mouths* and *four lips* mutations affect stomatal production in *Arabidopsis*. *Plant Cell* **7,** 2227–2239 (1995).
9. Berger, D. & Altman, T. A subtilisin-like serine protease involved in the regulation of stomatal density and distribution in *Arabidopsis thaliana*. *Genes Dev.* **14,** 1119–1131 (2000).
10. Todd, J., Post-Beittenmiller, D. & Jaworski, J. G. *KCS1* encodes a fatty acid elongase 3-ketoacyl-CoA synthase affecting wax biosynthesis in *Arabidopsis thaliana*. *Plant J.* **17,** 119–130 (1999).
11. Lassner, M. W., Lardizabal, K. & Metz, J. G. A jojoba β-keto-CoA synthase cDNA complements the canola fatty acid elongation mutation in transgenic plants. *Plant Cell* **8,** 281–292 (1996).
12. Zeiger, E. & Stebbins, L. Developmental genetics in barley: a mutant for stomatal development. *Am. J. Bot.* **59,** 143–148 (1972).
13. Jenks, M. A., Tuttle, H. A., Eigenbrode, S. D. & Feldmann, K. A. Leaf epicuticular waxes of the eceriferum mutants in *Arabidopsis*. *Plant Physiol.* **108,** 369–377, (1995).
14. Post-Beittenmiller, D. The cloned *Eceriferum* genes of *Arabidopsis* and the corresponding *Glossy* genes in maize. *Plant Physiol. Bioch.* **36,** 157–166 (1998).
15. Lolle, S. J., Cheung, A. Y. & Sussex, I. M. *fiddlehead*: an *Arabidopsis* mutant constitutively expressing an organ fusion program that involves interactions between epidermal cells. *Dev. Biol.* **152,** 383–392 (1992)
16. Lolle, S. J. *et al.* Developmental regulation of cell interactions in the *Arabidopsis fiddlehead–1* mutant: a role for the epidermal cell wall and cuticle. *Dev. Biol.* **189,** 311–321 (1997).
17. Yephremov, A. *et al.* Characterization of the *FIDDLEHEAD* gene of *Arabidopsis* reveals a link between adhesion response and cell differentiation in the epidermis. *Plant Cell* **11,** 2187–2201 (1999).
18. Larkin, J. C., Marks, M. D., Nadeau, J. & Sack, F. Epidermal cell fate and patterning in leaves. *Plant Cell* **9,** 1109–1120 (1997).
19. Bünning, E. & Sagromsky, H. Die Bildung des Spaltöffnungsmusters in der Blattepidermis. *Z. Naturforsch.* **3b,** 203–216 (1948).
20. Korn, R. W. Evidence in dicots for stomatal patterning by inhibition. *Int. J. Plant Sci.* **154,** 367–377 (1993).
21. Neighbour, E. A. *et al.* A small-scale controlled environment chamber for the investigation of effects of pollutant gases on plants growing at cool or sub-zero temperature. *Environ. Pollution* **64,** 155–168 (1990).
22. Jefferson, R. A. Assaying chimeric genes in plants: The *GUS* gene fusion system. *Plant Mol. Biol. Rep.* **5,** 387–405 (1987).
23. Beckman, A. A. & Engler, A. A. An easy technique for the clearing of histochemically stained plant tissue. *Plant Mol. Biol. Rep.* **12,** 37–42 (1994).
24. Salisbury, E. J. On the causes and ecological significance of stomatal frequency with special reference to woodland flora. *Phil. Trans. R. Soc. Lond. B* **216,** 1–65 (1927).
25. Weyers, J. D. B. & Johansen, L. G. Accurate estimation of stomatal aperture from silicone rubber impressions. *New Phytol.* **101,** 109–115 (1985).
26. Poole, I., Weyers, J. D. B., Lawson, T. & Raven, J. A. Variations in stomatal density and index: implications for paleoclimatic reconstructions. *Plant Cell Environ.* **19,** 705–712 (1996).
27. Barthels, N. *et al.* Regulatory sequences of *Arabidopsis* drive reporter gene expression on nematode feeding structures. *Plant Cell* **9,** 2119–2134 (1997).
28. Lin, X. Y. *et al.* Sequence and analysis of chromosome 2 of the plant *Arabidopsis thaliana*. *Nature* **402,** 761–765 (1999).
29. Gleave, A. P. A versatile binary vector system with a T-DNA organisational structure conducive to efficient integration of cloned DNA into the plant genome. *Plant Mol. Biol.* **20,** 1203–1207 (1992).
30. Valvekens, D., Van Montagu, M. & Van Lijsebettens, M. *Agrobacterium tumefaciens*-mediated transformation of *Arabidopsis thaliana* root explants by using kanamycin selection. *Proc. Natl Acad. Sci. USA* **85,** 5536–5540 (1988).

Acknowledgements

We acknowledge the assistance of J. Proctor, J. Balk, A. G. Moir and P. Tripathi with this work. We would like to thank K. Lindsey and S. Bright for helpful discussions.

Correspondence and requests for materials should be addressed to A.M.H. (e-mail: A.Hetherington@lancaster.ac.uk). The accession numbers for ATTS 5501, FL30 and FL44 are in GenBank under accession numbers AF188484, AF188485 and AF188486, respectively.

The *ELF3 zeitnehmer* regulates light signalling to the circadian clock

Harriet G. McWatters*, Ruth M. Bastow*, Anthony Hall & Andrew J. Millar

Department of Biological Sciences, University of Warwick, Gibbet Hill Road, Coventry, CV4 7AL, UK

** These authors contributed equally to this work*

The circadian system regulates 24-hour biological rhythms[1] and seasonal rhythms, such as flowering[2]. Long-day flowering plants like *Arabidopsis thaliana*, measure day length with a rhythm that is not reset at lights-off[3], whereas short-day plants measure night length on the basis of circadian rhythm of light sensitivity that is set from dusk[2]. *early flowering 3* (*elf3*) mutants of *Arabidopsis* are aphotoperiodic[4] and exhibit light-conditional arrhythmia[5,6]. Here we show that the *elf3-7* mutant retains oscillator function in the light but blunts circadian gating of *CAB* gene activation, indicating that deregulated phototransduction may mask rhythmicity. Furthermore, *elf3* mutations confer the resetting pattern of short-day photoperiodism, indicating that gating of phototransduction may control resetting. Temperature entrainment can bypass the requirement for normal *ELF3* function for the oscillator and partially restore rhythmic *CAB* expression. Therefore, *ELF3* specifically affects light input to the oscillator, similar to its function in gating *CAB* activation, allowing oscillator progression past a light-sensitive phase in the subjective evening. *ELF3* provides experimental demonstration of the *zeitnehmer* ('time-taker') concept[7,8].

As *elf3* mutants are rhythmic in darkness (DD)[5,6], ELF3 cannot be an essential component of the circadian oscillator. We tested whether the apparent arrhythmia in constant light (LL) of *elf3* plants was in fact masking an underlying oscillation. We entrained wild-type, null mutant *elf3-1* and partial mutant *elf3-7* (refs 5, 6) plants to light/dark cycles (LD), transferred them to LL and released replicate samples into DD at 2-h intervals, monitoring the phase of *CAB* expression in DD to determine the state of the oscillator in the preceding LL interval. We reasoned that if an underlying oscillator in the *elf3* mutants was masked by constant illumination, its phase should be reflected in the phase of the peak in DD. If the oscillator were dysfunctional in *elf3* mutants under LL, the timing of the *CAB*

peak would be determined by the time at which the plants were transferred to darkness.

In wild-type plants, the timing of the *CAB* peak after the light to dark transition remains under circadian control (Fig. 1a), occurring at or immediately preceding the phases predicted from the entraining LD cycle (roughly 4, 28 or 52 h after lights-on). The circadian system was stably entrained to the LD cycles, continued to oscillate during the 2 d of LL and was little affected by the last light to dark transition. *elf3-1* shows no evidence of circadian regulation after 10 h or more of light (Fig. 1a), as the phase of peak *CAB* expression is determined by the time of transfer to DD. The peak occurs after 9–12 h in darkness, indicating that the oscillator resumes from a phase equivalent to 8–11 h after lights-on. This pattern is strikingly similar to the photoperiodic response rhythm of short-day plants[2]. *elf3-7* showed an intermediate phenotype, retaining circadian-regulated *CAB* expression with a phase closer to wild type for up to 14 h of LL (Fig. 1b; up to 20 h in a minority of plants, data not shown). After this interval, the transfer to DD determined the peak phase, as in *elf3-1*. Partial *ELF3* function (in *elf3-7*) therefore maintained rhythmicity during the first 14 h of LL. The absence of *ELF3* (in *elf3-1*) resulted in a circadian oscillator that functioned still more briefly and abnormally in LL. We revealed a functional oscillator in *elf3-7* during the first 14 h of LL, by testing circadian rhythms in DD, whereas directly testing *CAB* expression under LL showed complete arrhythmia[6]. We conclude that the *CAB* output rhythm is masked during the first subjective day in LL, but that the oscillator is dysfunctional thereafter.

Continuous acute activation of *CAB* expression in response to continuous light might cause such masking. We therefore directly monitored the acute response to light in *elf3* mutants grown in LD 12/12 and transferred to DD (Fig. 2). Replicate samples that were exposed to 20 min light at 2-h intervals showed a rhythm of responsiveness to light in the wild type, with little or no acute response during the first and second subjective nights and large responses during the subjective day (as previously reported[9]). The *elf3* mutants had lost the normal circadian gating, showing strong acute responses throughout the first subjective night. In *elf3-1* in particular, the level of the acute response is increased during the subjective day. A low-amplitude modulation of the acute response is preserved during the first subjective night, but after 30 h the *CAB* activation levels are constant in both *elf3* mutants, indicating a complete absence of circadian gating. The gating defect of *elf3-7* suggests that the misregulated acute response activated *CAB* continuously in LL, masking the functional circadian oscillator. The extent of masking of the circadian system might be determined through the expression of genes such as *CCR2*, which are regulated by the clock but not light.

The high-amplitude rhythms of *CAB* expression in wild-type plants under LL therefore depend on circadian gating of light responsiveness in the late subjective day and early subjective night. The term *zeitnehmer* ('time-taker') has been applied to an input pathway rhythmically regulated by feedback from an oscillator, thus creating rhythmic input even under constant conditions[10,11]. The gating defect of even the partial loss-of-function *elf3-7* mutant suggests that high levels of *ELF3* are required for a normal gating function. The *elf3* mutations also result in a non-sustainable oscillator in LL, with a partial defect allowing progression to the mid-subjective night and the severe loss-of-function of *elf3-1* losing rhythmic control more rapidly. We propose that *ELF3* does not function directly in the circadian oscillator, but gates light input to the oscillator, allowing oscillator progression through a light-sensitive phase around dusk. A defect in the circadian gating of

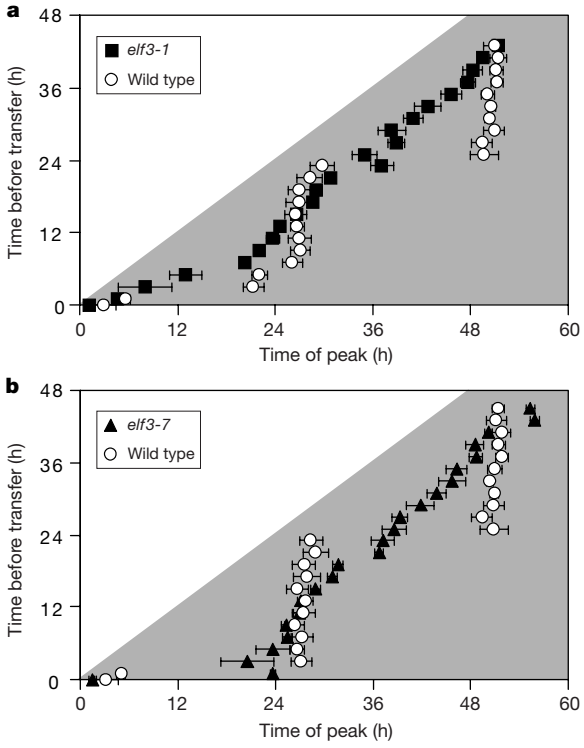

Figure 1 Timing of *CAB–LUC* peaks after LD cycles. **a**, *elf3-1* and its wild-type parent, gl1. **b**, *elf3-7* and its wild-type parent, 424. All plants were entrained to LD 12/12 for 6 d. At ZT 0, subjective dawn, plants were transferred to bright LL at 22 °C. Plants were transferred to darkness at 2-h intervals starting at subjective dawn; scintillation counter assays began at the time of transfer. White area represents the length of time plants spent in constant light before being transferred to the dark. Data are representative of two independent experiments; mean ± s.e.m. is shown, $n = 10–16$.

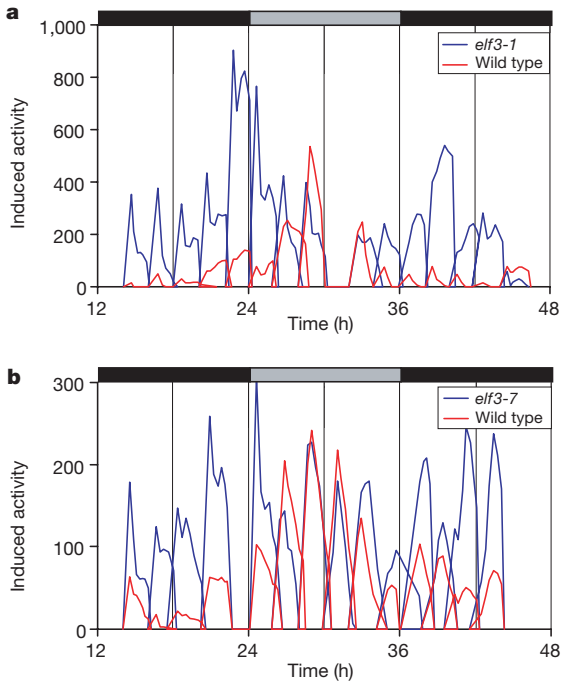

Figure 2 Circadian modulation of the acute response to light in *elf3* mutants. **a**, *elf3-1* and its wild-type parent, gl1. **b**, *elf3-7* and its wild-type parent, 424. All plants were entrained to LD 12/12 for 6 d. At ZT 12 on day 6, plants were transferred to DD. Replicate samples were then exposed to a 20-min white-light pulse every 2 h. Luminescence was measured both before and after the light treatment. The mean resulting induction of *CAB–LUC* luminescence was calculated by subtraction of the basal luminescence level of individual seedlings ($n = 24$) before the light treatment. Light and dark shading represents subjective day and subjective night, respectively. Data are representative of three independent experiments.

phototransduction can account for both the masking and oscillator arrest phenotypes of *elf3* mutants. As *elf3* mutations are sufficient to confer strong resetting at lights off, the *ELF3 zeitnehmer* might in part determine the mode of daylength measurement. Our evidence for an oscillation in *elf3* plants under LL, albeit transitory and at an early phase, suggests that these mutants might respond differentially to short and very short photoperiods. We suggest that the *elf3* oscillator arrests in LL rather than oscillating in an altered state and being reset by the light to dark transition; the pattern of phases in DD does not show the periodic variation indicative of a light limit cycle[2].

Reasoning that a masked oscillator might be revealed by reducing the strength of the masking light signal, we entrained plants using LD cycles of low fluence light ($10\ \mu mol\ m^{-2}\ s^{-1}$) and assayed *CAB–LUC* activity in this fluence rate LL. Only wild-type plants exhibited free-running circadian rhythms: reducing fluence rate alone was insufficient to restore overt rhythmicity to *elf3* mutants (see Supplementary Information). We next replaced light with temperature entrainment as temperature cycles, but not light cycles, can entrain *frq* null strains of *Neurospora crassa*[8]. In low fluence light, wild-type plants entrained to temperature cycles. When released into constant conditions, plants continued rhythmically in a free-run from the original phase, with lower mean levels and lengthened period (τ = 25–26 h) (Fig. 3a), as described for dim LL[12]. Although circadian rhythms in both *elf3-1* and *elf3-7* plants could be driven by temperature cycles in LL they did not subsequently produce free-running circadian rhythms in bright or dim LL (Fig. 3a; and Supplementary Information); neither temperature nor light alone could rescue circadian behaviour under constant illumination.

As temperature cycles did not restore overt circadian rhythms of *CAB* expression in *elf3* under LL, we tested the phase of rhythms in DD to reveal the behaviour of the underlying oscillator. We entrained plants in temperature cycles in bright LL ($140\ \mu mol\ m^{-2}\ s^{-1}$), then released them into DD at constant temperature. As after light entrainment, wild-type plants showed circadian *CAB* expression peaks phased with respect to the (discontinued) temperature cycle, even after two days in constant conditions (Fig. 4). Thus, the wild-type oscillator was entrained by temperature and was not reset by a single light–dark transition. After transfer to darkness at the first subjective dawn, the phase of both *elf3-1* and *elf3-7* was identical to that of wild-type plants (Fig. 4). Previous experiments with LD cycles at constant temperature have shown that *elf3-7* has an earlier peak than wild type, with that of *elf3-1* being earlier still[5,6]. Thus temperature cycles, in contrast to light cycles (Fig. 2; and see ref. 6), entrained the *elf3* plants initially to a wild-type phase relationship.

This intriguing result implies that the *elf3* lesion specifically affects the light input pathway. During the first 5 h in constant conditions *elf3-1* showed an early phase when transferred to darkness, with a sharp jump to a later phase in plants transferred after 7–11 h, implying that an oscillator is still working for the first subjective day in constant conditions. Thereafter, *elf3-1* plants did not show circadian regulation: peaks of *CAB–LUC* expression were phased from the transfer to darkness (Fig. 4a), as after LD cycles (Fig. 2), suggesting the oscillator was no longer functional. In contrast to *elf3-1* and unlike its response to LD cycles, *elf3-7* showed a stable circadian pattern up to 48 h in LL (Fig. 4b). Thus an oscillator remains in *elf3-7* which may be entrained by tempera-

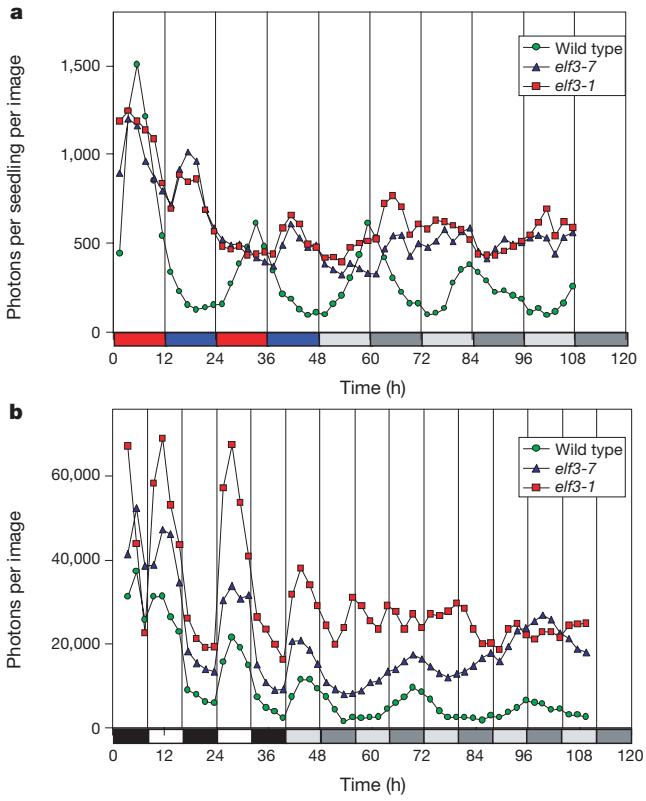

Figure 3 Response to temperature or combined light and temperature cycles. **a**, *CAB–LUC* activity in temperature cycles in low fluence LL ($10\ \mu mol\ m^{-2}\ s^{-1}$). T-cycle = 24 h: 'day' is 12 h at 24 °C, 'night' is 12 h at 18 °C. After measuring luminescence for 48 h, temperature cycles were discontinued and plants were placed in dim LL, 22 °C for the remainder of the assay. Data are representative of four independent experiments. Red and blue bars represent warm and cold periods, respectively; light and dark shading represents subjective day and subjective night, respectively. **b**, *CAB–LUC* activity in simultaneous light and temperature cycles. T-cycle = 16 h: 'day' is 8 h dim light ($10\ \mu mol\ m^{-2}\ s^{-1}$) at 24 °C, 'night' is 8 h dark at 18 °C. After T-cycle entrainment, plants were transferred to dim LL, 22 °C at subjective dawn. Data are representative of two independent experiments. White and black bars represent light and darkness, respectively. Light and dark shading represents subjective day and subjective night, respectively.

ture cycles and free-run in constant conditions (Fig. 3a). The output of this covert oscillator is easily masked, even by dim light, leading to overt arrhythmia. In contrast, the *elf3-1* oscillator stops within 12 h of constant light.

We reasoned that since circadian timing in *elf3-7* is restored after temperature cycles, light and temperature cycles together could reinforce circadian function. We combined these two *zeitgebers* to produce warm days and cooler nights. We used various entraining periods (T-cycles) as the earlier phase of *elf3* after LD cycles can be interpreted as a short endogenous period. No genotype free-ran after 12-h T-cycles (data not shown). Wild-type plants showed free-running rhythmicity after 16-h T-cycles (Fig. 3b) or after 24-h T-cycles (see Supplementary Information). Entrainment to combined low light and temperature cycles of 16, 20 or 24 h restored free-running rhythmicity in a minority of samples of *elf3-1* and *elf3-7* plants (Fig. 3b). In two independent experiments, 3 out of 28 samples of *elf3-1* and 10 out of 29 samples of *elf3-7* free-ran after such cycles with periods of around 26 h (judged free-running if FFT-NLLS analysis returned a period of 15–35 h with a relative amplitude error less than 0.6; ref. 13) (Fig. 3b). In comparison, after entrainment to a single *zeitgeber*, either light or temperature, none out of 40 *elf3-1* samples and 1 out of 40 *elf3-7* samples free-ran (Fig. 3a; and Supplementary Information). In contrast, all wild-type controls entrained to a single *zeitgeber* were rhythmic (40 out of 40 samples); 47 out of 57 samples were rhythmic after combined light and temperature entrainment. The free-running periods obtained in *elf3* were not distinguishable from those of wild-type plants: the long period is attributed to the low light intensity. Reinforcing the entraining effects of temperature with low-amplitude light cycles can overcome the masking effects of light on the circadian system in *elf3* plants to reveal the underlying oscillator despite ongoing illumination.

Our results indicate that despite their common arrhythmia in LL[5,6], the circadian system of *elf3-7* is less compromised than that of *elf3-1*. We suggest *elf3-1* is arrhythmic because its circadian system arrests rapidly in LL, although it is capable of restarting from a constant phase in darkness. In contrast, *elf3-7* plants retain sufficient ELF3 function to maintain (masked) oscillations for at least 2 d in constant light. Their oscillator can be rescued and free-running rhythmicity restored by prior entrainment by temperature, especially if masking is reduced by low light intensity. The different responses of *elf3-7* to light or temperature cycles indicate that the *elf3* lesion affects a light input pathway, rather than the temperature-sensitive oscillator. The gating of the acute response of *CAB* in the early to mid night (*zeitgeber* time (ZT) 12–16) coincides with the arrest of the oscillator in *elf3-7* (*circa* ZT 14) after light and *elf3-1* (*circa* ZT 11) after temperature cycles; this is also the phase from which their oscillators restart in darkness. This strongly implies that *ELF3* functions at this phase of the circadian cycle. A rhythmic *ELF3*-dependent antagonism of the phototransduction pathway to the clock and to *CAB* at this phase can account for all the *elf3* phenotypes. Our data provide empirical evidence for the *zeitnehmer* ('time-taker') concept[10]: we show that *ELF3* is a part of the *zeitnehmer* feedback loop necessary to maintain self-sustained oscillations rather than an oscillator component. □

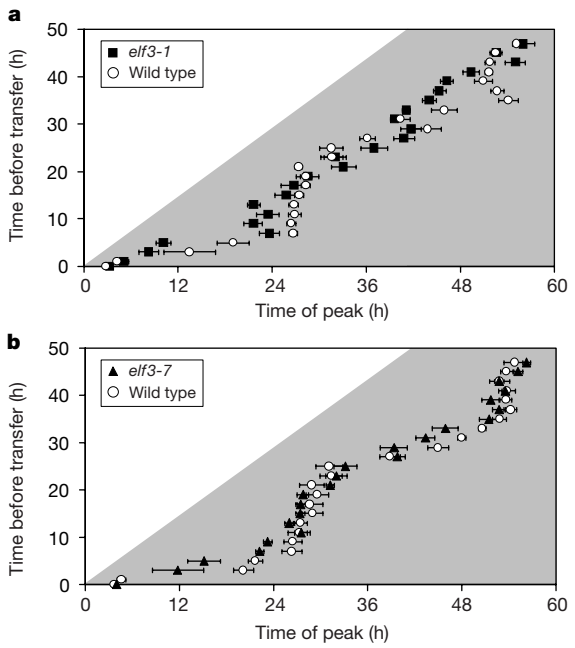

Figure 4 Timing of *CAB–LUC* peaks after temperature cycles. **a**, *elf3-1* and its wild-type parent, gl1. **b**, *elf3-7* and its wild-type parent, 424. All plants were entrained to 12 h at 24 °C, 12 h of 18 °C temperature cycles in high fluence LL (140 μmol m^{-2} s^{-1}) for 6 d. From ZT 0, subjective dawn, plants were maintained in bright LL at 22 °C. Plants were transferred to darkness at 2-h intervals starting at subjective dawn; scintillation counter assays began at the time of transfer. White area represents the length of time plants spent in constant light before being transferred to the dark. Data are representative of two independent experiments; mean ± s.e.m. is shown, $n = 10–16$.

Methods

Plant materials and growth conditions

Transgenic *A. thaliana* containing the *CAB–LUC* fusion together with the *elf3-1* mutation in the Columbia *gl1* background or with the *elf3-7* mutation in the Columbia-0 background have been described[5,6]. In all cases wild type refers to the respective parent. Seeds were imbibed then stratified (48 h at 4 °C) on solid Murashige and Skoog (MS) medium with 3% sucrose[14].

Entrainment conditions

After imbibition and stratification as described above[14], seedlings were entrained for 6 d in light/dark and/or temperature cycles as appropriate in controlled environment chambers (Percival or Sanyo) before measurements began. Constant light or LD cycles involved high fluence fluorescent light (140 μmol m^{-2} s^{-1}) (Figs 1 and 4) or low fluence fluorescent light (10 μmol m^{-2} s^{-1}) (Fig. 3). Light pulses were 80 μmol m^{-2} s^{-1} (Fig. 2). Constant temperature was 22 °C. Temperature cycles consisted of warm periods (24 °C) and cold periods (18 °C).

Bioluminescence assay

Luminescence levels of individual seedlings were measured in a Packard Topcount[15]. Luminescence of groups of seedlings ($n = 30–100$) was measured by low-light video imaging using a liquid nitrogen cooled camera (Princeton Instruments)[16,17] and normalized for seedling number[9]. Instrument background has been subtracted from the data presented.

Received 30 June; accepted 1 September 2000.

1. Dunlap, J. C. Molecular bases for circadian clocks. *Cell* **96,** 271–290 (1999).
2. Lumsden, P. J. in *Biological Rhythms and Photoperiodism in Plants* (eds Lumsden, P. J. & Millar, A. J.) 167–181 (BIOS Scientific, Oxford, 1998).
3. Samach, A. & Coupland, G. Time measurement and the control of flowering in plants. *BioEssays* **22,** 38–47 (2000).
4. Zagotta, M. T., Shannon, S., Jacobs, C. & Meeks-Wagner, D. R. Early-flowering mutants of *Arabidopsis thaliana*. *Aust. J. Plant Physiol.* **19,** 411–418 (1992).
5. Hicks, K. A. *et al.* Conditional circadian dysfunction of the *Arabidopsis early-flowering 3* mutant. *Science* **274,** 790–792 (1996).
6. Reed, J. W. *et al.* Independent action of ELF3 and phyB to control hypocotyl elongation and flowering time. *Plant Physiol.* **122,** 1149–1160 (2000).
7. Roenneberg, T. & Merrow, M. Molecular circadian oscillators: An alternative hypothesis. *J. Biol. Rhythms* **13,** 167–179 (1998).
8. Merrow, M., Brunner, M. & Roenneberg, T. Assignment of circadian function for the *Neurospora* clock gene *frequency*. *Nature* **399,** 584–586 (1999).
9. Millar, A. J. & Kay, S. A. Integration of circadian and phototransduction pathways in the network controlling *CAB* gene transcription in *Arabidopsis*. *Proc. Natl Acad. Sci. USA* **93,** 15491–15496 (1996).
10. Roenneberg, T. & Merrow, M. Circadian systems and metabolism. *J. Biol. Rhythms* **14,** 449–459 (1999).
11. Lakin-Thomas, P. L. Circadian rhythms: new functions for old clock genes? *Trends Genet.* **16,** 135–142 (2000).
12. Somers, D. E. & Quail, P. H. Phytochrome-mediated light regulation of *PHYA*- and *PHYB*-GUS_ transgenes in *Arabidopsis thaliana* seedlings. *Plant Physiol.* **107,** 523–534 (1995).
13. Dowson-Day, M. J. & Millar, A. J. Circadian dysfunction causes aberrant hypocotyl elongation patterns in *Arabidopsis*. *Plant J.* **17,** 63–71 (1999).
14. Millar, A. J., Carré, I. A., Strayer, C. A., Chua, N. H. & Kay, S. A. Circadian clock mutants in *Arabidopsis* identified by luciferase imaging. *Science* **267,** 1161–1163 (1995).
15. Carré, I. A. & Kay, S. A. Multiple DNA–protein complexes at a circadian-regulated promoter element. *Plant Cell* **7,** 2039–2051 (1995).

16. Bognar, L. K. *et al.* The circadian clock controls the expression pattern of the circadian input photoreceptor, phytochrome B. *Proc. Natl Acad. Sci. USA* **96,** 14652–14657 (1999).
17. Millar, A. J., Short, S. R., Chua, N. H. & Kay, S. A. A novel circadian phenotype based on firefly luciferase expression in transgenic plants. *Plant Cell* **4,** 1075–1087 (1992).

Supplementary information is available on *Nature's* World-Wide web site (http://www.nature.com) or as paper copy from the London editorial office of *Nature*.

Acknowledgements

R.M.B. was supported by a Gatsby graduate studentship; this work was supported by grants from the BBSRC to A.J.M.

Correspondence and requests for materials should be addressed to A.J.M. (e-mail: Andrew.Millar@warwick.ac.uk).

μ-Opioid receptor desensitization by β-arrestin-2 determines morphine tolerance but not dependence

Laura M. Bohn*, Raul R. Gainetdinov*, Fang-Tsyr Lin†, Robert J. Lefkowitz† & Marc G. Caron*

** Howard Hughes Medical Institute Laboratories, Departments of Cell Biology and Medicine, Duke University Medical Center, Durham, North Carolina 27710, USA*

† Howard Hughes Medical Institute Laboratories, Departments of Biochemistry and Medicine, Duke University Medical Center, Durham, North Carolina 27710, USA

Morphine is a powerful pain reliever, but also a potent inducer of tolerance and dependence. The development of opiate tolerance occurs on continued use of the drug such that the amount of drug required to elicit pain relief must be increased to compensate for diminished responsiveness[1–3]. In many systems, decreased responsiveness to agonists has been correlated with the desensitization of G-protein-coupled receptors. *In vitro* evidence indicates that this process involves phosphorylation of G-protein-coupled receptors and subsequent binding of regulatory proteins called β-arrestins[4,5]. Using a knockout mouse lacking β-arrestin-2 (βarr2$^{-/-}$), we have assessed the contribution of desensitization of the μ-opioid receptor to the development of morphine antinociceptive tolerance and the subsequent onset of physical dependence. Here we show that in mice lacking β-arrestin-2, desensitization of the μ-opioid receptor does not occur after chronic morphine treatment, and that these animals fail to develop antinociceptive tolerance. However, the deletion of β-arrestin-2 does not prevent the chronic morphine-induced up-regulation of adenylyl cyclase activity, a cellular marker of dependence, and the mutant mice still become physically dependent on the drug.

We have shown previously[6] that morphine-induced antinociception is enhanced and prolonged in mice lacking β-arrestin-2. This perpetuation of morphine analgesia suggests that mice lacking β-arrestin-2 may be resistant to the desensitization of the morphine signal. As specific inhibitors of desensitization do not exist, this genetically altered animal model provides a means to potentially abrogate desensitization of the μ-opioid receptor (μOR) in response to morphine. Thus, we examined the regulation of the μOR in relationship to the development of morphine tolerance and dependence in βarr2$^{-/-}$ mice.

An acute challenge with a high dose of morphine induces acute morphine antinociceptive tolerance 24 h after the initial challenge. In this scheme, mice are assessed for their nociceptive response latencies after a moderate dose of morphine (10 mg per kg, subcutaneously (s.c.)) 24 h after receiving an injection of either saline or 100 mg per kg morphine. Indicative of antinociceptive tolerance, wild-type mice exhibited a roughly 50% reduction in morphine responsiveness if they had received morphine, as compared to saline, the day before (Fig. 1a). The βarr2$^{-/-}$ mice maintained the same degree of responsiveness to morphine, however, whether they had been treated with saline or morphine on the previous day. It therefore seemed that the βarr2$^{-/-}$ mice did not develop acute antinociceptive tolerance to morphine.

As, in the clinical setting, tolerance to morphine's analgesic properties usually develops over continued use of moderate levels of the drug, we evaluated the analgesia provided after daily administration of morphine. Mice were injected daily with morphine, and paw-withdrawal latencies were recorded (Fig. 1b). Although the wild-type littermates had significantly diminished responsiveness to the drug by day 5, the knockout mice continued to experience as much antinociception on day 5 to day 9 as on day 1. To characterize this resistance to morphine antinociceptive tolerance in the βarr2$^{-/-}$

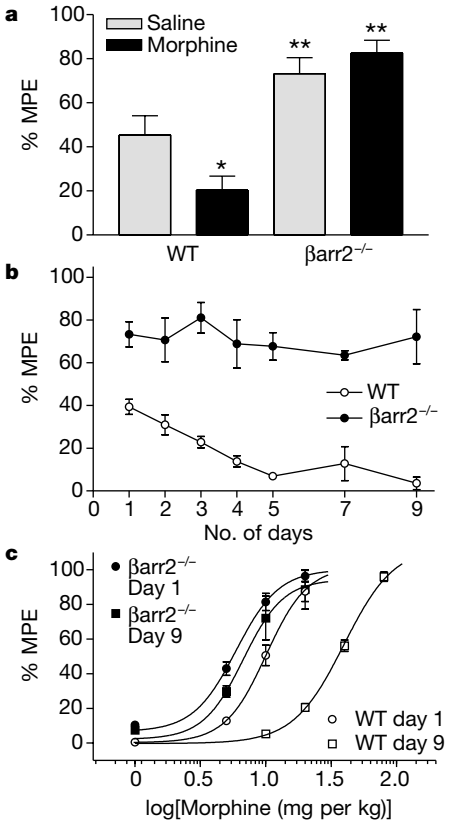

Figure 1 Lack of morphine antinociceptive tolerance in βarr2$^{-/-}$ mice. **a**, Acute tolerance. Wild-type (WT) and βarr2$^{-/-}$ mice were treated with either saline or morphine (100 mg per kg, s.c.). After 24 h, mice were treated with morphine (10 mg per kg, s.c.) and hot-plate-response latencies (56 °C) were recorded. Data are presented as the mean ± s.e.m., $n = 7–8$. Asterisk, $P < 0.05$ versus WT + saline; two asterisks, $P < 0.05$ versus WT, Student's *t*-test. **b**, Chronic tolerance. Mice were treated daily with morphine (10 mg per kg, s.c.); antinociception was assessed 30 min after the injection on the days indicated. Means ± s.e.m. are shown. $P < 0.0001$, WT versus βarr2$^{-/-}$; two-way analysis of variance (ANOVA). **c.** Chronic tolerance. Dose–response curves were determined using a cumulative dosing scheme on day 1 and day 9. On day 1, both genotypes were treated with 1, 5, 10 and 20 mg per kg, s.c. On day 9, βarr2$^{-/-}$ mice ($n = 6–12$) were again challenged with this same dose scheme, whereas WT ($n = 7–14$) were cumulatively treated with 10, 20, 40 and 80 mg per kg, s.c. and βarr2$^{-/-}$. Means ± s.e.m. are shown. ED_{50} (50% effective dose) values were calculated by nonlinear regression analysis (GraphPad Prism); 95% confidence intervals: day 1: WT, 10.1 (8.4–12.1); βarr2$^{-/-}$, 5.9 (5.0–7.0); day 9: WT, 39.6 (34.0–46.1); βarr2$^{-/-}$, 6.7 (4.8–9.3).